Paste 2023 – GW Wilson, NA Beier, DC Sego, AB Fourie & D Reid (eds)

doi:10.36487/ACG_repo/2355_17

Prediction of the mechanical properties of cemented paste backfill using artificial intelligence approaches

M Amri *Université du Québec en Abitibi-Témiscamingue, Canada*

T Belem *Université du Québec en Abitibi-Témiscamingue, Canada*

H Mrad *Université du Québec en Abitibi-Témiscamingue, Canada*

LP Gélinas *Agnico Eagle Mines Ltd, Canada*

F Masmoudi *National School of Engineering of Sfax, Tunisia*

Abstract

In the digital era, the mining industry benefits from powerful tools that can help to optimise underground backfilling operations and to increase overall safety. Indeed, with current progress in artificial intelligence (AI), machine learning (ML) creates state-of-the-art techniques in the mining sector that could significantly improve the productivity and efficiency of mining operations. The purpose of this study is to apply ML algorithms, including the gradient boosting regressor (GBR), the XGBoost regressor (XGBR), and the support vector regressor (SVR) to predict the uniaxial compressive strength (UCS) of cemented paste backfill (CPB). A total of 1,587 UCS data were used to train the ML algorithms, considering different variables such as the types of tailings, binder and their proportion, solid mass concentration, slump height, water quality, and curing time. The raw data were pre-processed before training the models, as well as their hyperparameters tuning was made by a random search method followed by 4-fold cross-validation. The prediction results show that the GBR algorithm is the most powerful one which has a coefficient of correlation (R) between predicted and experimental values equal to 0.99 and a root-mean-square error (RMSE) equal to 0.16. This prediction is validated through new-lab prepared CPB specimens.

Keywords: *artificial intelligence, machine learning, database, prediction models, uniaxial compressive strength, cemented paste backfill*

1 Introduction

Public commitment and recent environmental legislation are becoming increasingly stringent and are constraining mining companies to follow the 'towards sustainable mining' standard, which is a globally recognised sustainability program in managing key environmental and social risks of their solid waste storage facilities.

In the case of underground operations, the formulation of mine backfill using these solid wastes is the most widespread approach, not only for filling the underground excavations produced during ore extraction to ensure the ground stability, but also for reducing the huge quantities of mine waste to be stored on surface. Among the most used worldwide types of mine backfill is the cemented paste backfill (CPB) (e.g. Belem et al. 2003) which is made of tailings, a binding agent (e.g. general use Portland GU cement alone, or a blend of GU with ground granulated blast furnace slag, fly ash, etc.) and mixing water. CPB may also contain chemical admixtures such as superplasticisers (e.g. Ouattara 2017).

For this purpose, knowledge of the mechanical properties of CPB is essential for the implementation of a backfilling system. In practice, uniaxial compressive strength (UCS) is the most used parameter to evaluate the mechanical performance of CPB (e.g. Belem et al. 2003). Various empirical models have been developed to predict the UCS of mine backfill (e.g. Mitchell & Wong 1982; Arioglu 1984; Swan 1985; Lamos & Clark 1989; Yu 1989), but they are still complex and ignore all the physicochemical properties of the backfill

ingredients (i.e. tailings, binder, and mixing water). Other researchers have correlated the UCS with the shear wave velocity using non-destructive tests (ultrasonic pulse velocity [UPV]) (Ercikdi et al. 2014; Yılmaz & Ercikdi 2016), but this method is not robust and has not been well-developed.

More recently, the prediction of the UCS using advanced methods considering the influential parameters (proportion of cement and tailings, solid content, and curing time) has been developed in some studies. Qi et al. (2018a) developed an artificial neural network (ANN) combined with a particle swarm optimization (PSO) algorithm to predict the uniaxial compressive strength of CPB. A total of 396 tests were performed to build the dataset which contains only the types of tailings, cement-to-tailings ratio, solid content, and curing time (3, 7 and 28 days) as input data for the ANN. The prediction coefficient of correlation obtained was 0.979.

Yu et al. (2021) also used ANN, a support vector machine (SVM) model, and a salp swarm algorithm (SSA) optimisation algorithm as prediction methods to predict the UCS of CPB reinforced with polypropylene fibres. The dataset used for model training contains 720 UCS tests, cement-to-tailings ratio, solids content, curing time, fibres content, and fibres length were used as input data. The best prediction model ANN combined with the optimisation algorithm: SSA-ELM gave a coefficient of determination (R^2) compared to the test data of 0.94 and a root-mean-square error (RMSE) of 0.18.

Lu et al. (2019) combined a machine learning (ML) algorithm gradient boosting regression (GBR) with a PSO optimisation algorithm to predict the UCS, of which they used 126 UCS tests from specimens prepared using two types of tailings and the input data that were selected are cement-to-tailings ratio (0.083 to 0.25), solids content (66% to 78%), curing time (3, 7, 14 and 28 days). The prediction score obtained using this algorithm was R = 0.9837.

Qi et al. (2018b) used a slightly larger dataset of 1,077 UCS tests and 231 uniaxial tensile strength (UTS) tests to predict the properties of CPB, such as UCS, UTS, elastic modulus, and Young's modulus. They used the genetic algorithm for hyperparameters optimisation and three ML algorithms for the prediction: (i) decision tree (DT), (ii) gradient boosting machine (GBM), and (iii) random forest (RF). The results show that the GBM algorithm performs best, giving a correlation coefficient R = 0.963.

Mine backfill performance is sensitive to many factors such as the types and the proportion of binder, the mixing water amount and chemistry, the sulphides content, the physicochemical, and the mineralogical properties of the tailings. All the above-mentioned studies have not considered these factors in the database for model learning. Moreover, some mining conditions will require long-term UCS (from 90 to 360 days) data to satisfy the technical requirements of the operations. Long-term curing ages were not considered in any of the cited studies in this paper. The performance of learning algorithms depends strongly on the quantity of data provided (the more data used, the better their performances will be).

Most of the research studies on the prediction of the UCS used small datasets (less than 1,000 UCS tests). However, chemical additives can improve the UCS, GU-Slag compound binder develops much better strengths than GU cement (Sahi 2016). Most of the research has used only one type of binder, which is Portland cement. This shows a lack of diversity in the input data; also, only one type of water has been used (tap water) for the mix recipes formulation.

To remedy the limitations cited in the literature, the present study aims to use advanced ML algorithms for predicting the UCS of CPB based on an extensive dataset containing 1,587 UCS tests. The model predictions will be compared to the existing dataset and evaluated through laboratory tests to select the best-performing model.

2 Methodology

2.1 Materials characterisation

In this study, the ingredients used for the formulation of the CPB were tailings samples from three hard rock mines located in Abitibi-Témiscamingue region in Québec, Canada (namely, T1 = LaRonde mine tailings,

T2 = Westwood mine tailings, and T3 = Casa Berardi mine tailings), 15 types of hydraulic binder (GU Portland cement, Slag-blended, type F Fly ash-blended, and type C Fly ash-blended), and different types of water quality (tap water, lake water, and different concentration of sulphated water that are used by the mines).

The tailings used were first homogenised, then their relative density (G_s) was measured using a helium pycnometer AccuPyc II 1340 from Micromeritics. Their particle size distributions (PSD) were determined using a Mastersizer 3000 laser diffraction particle size analyser from Malvern Panalytical. The PSD curves for the three tailings samples from the three mines are presented in Figures 1, 2 and 3. The mineralogical analysis of these tailings was performed using X-ray diffraction. The physical characteristics and the mineralogical composition of the tailing's samples are summarised in Table 1.

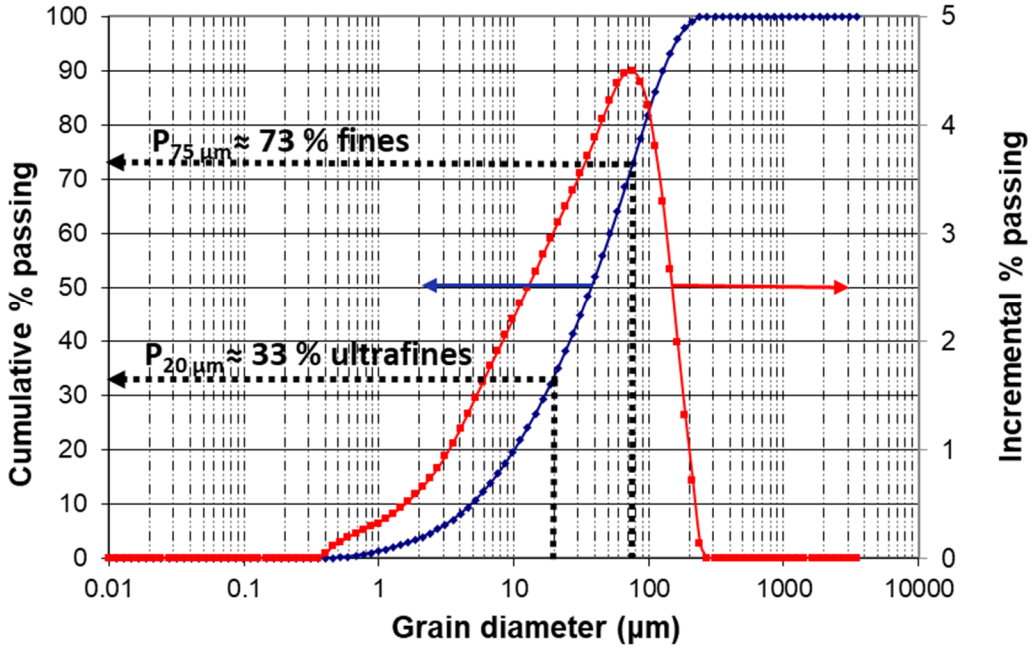

Figure 1 Particle size distribution curve of the LaRonde mine tailings

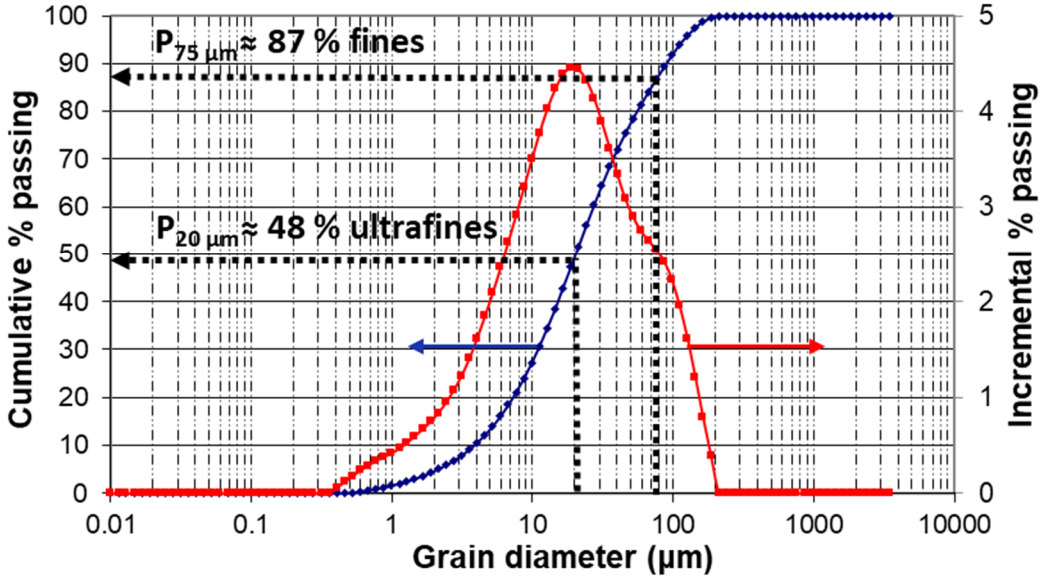

Figure 2 Particle size distribution curve of the Westwood mine tailings

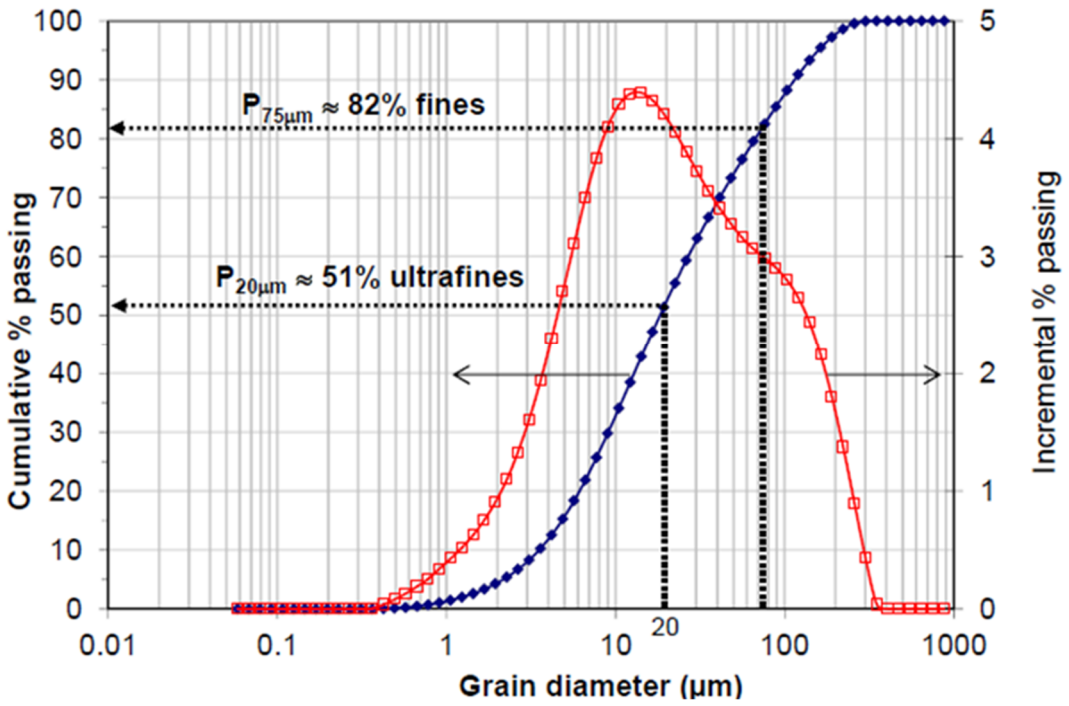

Figure 3 Particle size distribution curve of the Casa Berardi mine tailings

Table 1 Physical properties and mineralogical composition of the three tailings samples

Tailings sample	Physical properties				Mineralogical composition (%)			
	Gs	D_{10} (µm)	D_{90} (µm)	P_{20} µm (%)	Quartz	Pyrite	Chlorite	Muscovite
T1	3.18	4.9	127.0	33	56.2	18.6	5.0	6.2
T2	2.82	3.8	89.3	48	47.8	7.7	22.1	0.7
T3	2.80	3.6	120.7	51	34.8	2.7	12.3	22.7

2.2 Cemented paste backfill mixtures preparation

As previously mentioned, the CPB was obtained by mixing the tailings, binding agent, and water using a Hobart electric mixer (model D 300-1) for 5 to 7 minutes to homogenise the final paste. The different mixtures obtained were poured into plastic moulds (76 mm in diameter and 152 mm height), then sealed with their lids and stored in a room with a relative humidity of 90% and a temperature of 23± 2°C.

Using the three mine tailings samples and varying the type of binding agent and its proportion (binder ratio $B_w = M_{binder}/M_{dry\text{-}tailings}$), the type of water (tap, lake, sulphated), the mass solid percentage ($C_w = M_{solids}/M_{bulk}$), and the curing time, a total of 1,587 specimens were prepared (Table 2). In Table 2, xGU means x% GU, ySlag means y% Slag, and FA-C means type C fly ash.

Table 2 Experimental program for the CPB mixtures preparation

Tailings	Mass solid percentage C_w (%)	Types of binder	Binder ratio B_w (%)	Water quality	Curing time (days)
T1, T2, T3	64 to 88	10GU/90Slag 20GU/80Slag 30GU/70Slag 40GU/60Slag 40GU/60FA-C 50GU/50FA-C 60GU/40FA-C 57GU/43FA-C 70GU/30FA-C 100 GU	1 to 9	Tap water Lake water Sulphated water (2,500 ppm SO_4^{2}) Sulphated water (5,000 ppm SO_4^{2-})	1 to 213

2.3 Backfill mixes slump measurement

The fresh paste backfill slump height was determined using the standard Abrams cone (Figure 4), which is the most widely used due to the simplicity of its implementation. This test consists of filling the cone in three layers pounded 25 times by a metal rod, and then the cone is delicately lifted (about 4 seconds) in accordance with ASTM C143 (ASTM International 2020). The slump measured was between 6 and 9 in (152 and 229 mm) which corresponds to the typical slump of a paste fill (Landriault et al. 1997).

Figure 4 Slump measurement using the standard Abrams cone method

2.4 Uniaxial compression tests

The uniaxial compression tests were performed using a stiff mechanical press MTS 10/GL with a maximum capacity of 50 kN and run at a constant displacement velocity of 1 mm/min (Figure 5) according to ASTM C39 (ASTM International 2021). The tests were carried out in triplicate and a data acquisition system recorded the axial strain and the normal stress applied to the specimens during the test, which allows representing the

stress-strain curve and the maximum/peak value which corresponds to the UCS. Note that each UCS value at each curing time is obtained by averaging three values (triplicate).

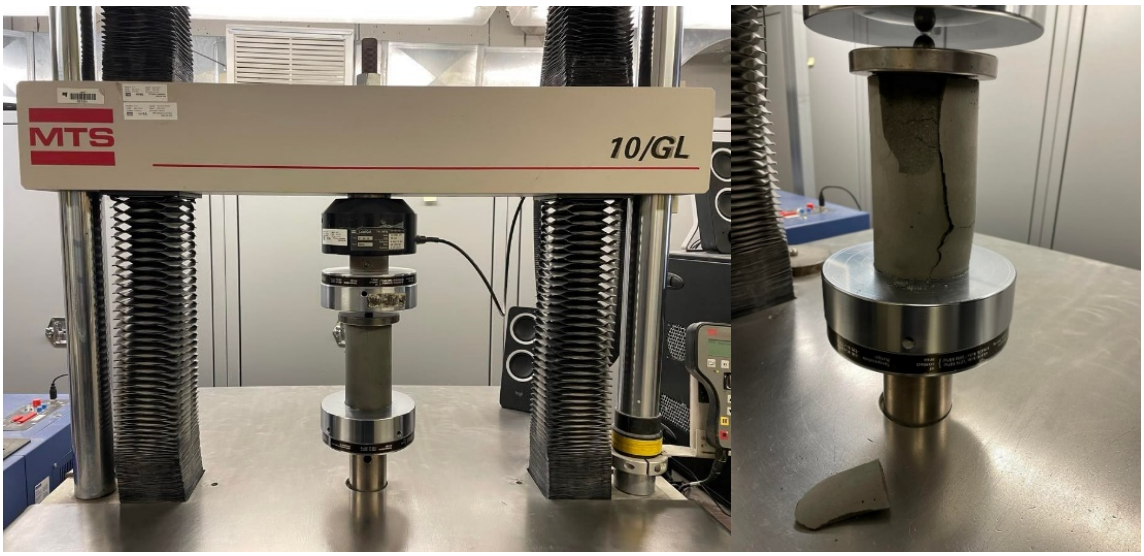

(a) (b)

Figure 5 Uniaxial compression test: (a) Stiff mechanical press MTS 10/GL; (b) Broken sample after test

2.5 Prediction methods using machine learning algorithms

The supervised ML process that has been adopted consists of first acquiring the data, processing them (deletion, discretisation, normalisation, preparation of categorical data if they exist etc.) and then splitting the data into two sets. In general, 70% are used for training the models and 30% to testing and validating the models (Nelson & Illingworth 1991; Nguyen et al. 2021). Second, model learning and hyperparameter tuning should be applied. Once the models are properly created and trained, evaluation and validation will be required afterward to select the best-performing one (Mathivet 2021).

In this paper, the data were collected from the results of 1,587 compression tests performed at the Unité de Recherche et de Service en Technologie Minérale Laboratory at the Université du Québec en Abitibi-Témiscamingue (UQAT), of which 17 features were selected as inputs for the models and the target was the UCS. The descriptive statistics of this data is presented in Table 3.

To improve the model learning, the data were scaled using the Robust scaler method by subtracting each value from the median and then dividing by the interquartile range (75% value – 25% value). This method effectively minimises the effect of outliers compared to other normalisation methods. Regarding the modeling, three ML models were chosen considering the dataset size, the type of data, and the data quality (Jakobowicz, 2021) to predict the UCS, namely the GBR, XGBoost regressor (XGBR) and support vector regression (SVR) (Pham et al. 2018; Qi et al. 2018a; Yaseen et al. 2018; Lu et al. 2019; Sun et al. 2020).

Table 3 Descriptive statistics of the data

Parameter	Count	Mean	Std	Min	25%	50%	75%	Max
G_s (–)	1,587	2.88	0.15	2.80	2.80	2.80	2.82	3.18
D_{10} (µm)	1,587	3.84	0.40	3.60	3.60	3.60	3.80	4.60
D_{90} (µm)	1,587	117.01	12.36	89.30	120.70	120.70	120.70	127.00
$P_{20µm}$ (%)	1,587	46.06	6.83	33.00	48.00	50.00	40.00	50.00
% Quartz	1,587	41.41	8.97	34.77	34.77	34.77	47.82	56.15
% Pyrite	1,587	6.87	6.36	2.68	2.68	2.68	7.67	18.60
% Chlorite	1,587	12.33	5.17	5.00	12.33	12.33	12.33	22.08
% Muscovite	1,587	15.63	9.27	0.66	6.20	22.66	22.66	22.66
Slump (inch)	1,587	7.37	0.54	6.25	7.00	7.00	8.00	9.00
Solids concentration (%)	1,587	71.52	2.63	63.90	70.00	72.50	73.23	87.80
GU cement (%)	1,587	39.82	23.87	10.00	20.00	30.00	60.00	100.00
Fly Ash_C (%)	1,587	8.45	18.15	0.00	0.00	0.00	0.00	60.00
Fly Ash_F (%)	1,587	9.20	19.41	0.00	0.00	0.00	0.00	70.00
Slag (%)	1,587	42.53	39.00	0.00	0.00	70.00	80.00	90.00
Binder ratio B_w (%)	1,587	5.28	1.60	1.00	4.5	4.50	7.00	9.22
Curing time (days)	1,587	44	34	1.00	14.00	28.10	56.00	213
UCS (kPa)	1,587	648.95	646.24	21.00	245.75	456.80	876.60	4,726.00

3 Results and discussion

3.1 Hyperparameters tuning of machine learning models

To avoid over-fitting and to find the optimal hyperparameters of the models, a random search method has been used in this study including *k*-fold cross-validation (k-CV). During the model training, random hyperparameter combinations were selected and then evaluated using cross-validation which consists of randomly dividing the training set into *k* subsets of which *k*-1 sets are dedicated for training and the remaining set is for validation (Qi et al. 2018a; Lu et al. 2019). The process of cross-validation will be repeated *k* times, and in this study, *k* was fixed to be 4 with the number of iterations (*n_iter*) equal to 10 which gives a total of 40 executions. Table 4 describes the optimal hyperparameters selected for the model learning.

Table 4 Description of the optimal hyperparameters

Model	Hyperparameters
GBR	*learning_rate* = 0.16, *max_depth* = 5, *min_samples_split* = 4, n_*estimators* = 613
XGBR	Subsample = 1, *n_estimators* = 800, *max_depth* = 12, *learning_rate* = 0.3, gamma = 0.1
SVR	C = 10^7, gamma = 10^{-5}

3.2 Performance evaluation and comparison of machine learning models

The performance evaluation of the models was done based on the linear coefficient of correlation (R), which determines the correlation between the predicted and the actual values. The closer the R-value is to 1, the more accurate the prediction will be. The RMSE measures the prediction error rate on a (N) dataset. These two metrics are defined as follows:

$$R = \frac{\sum_{i=1}^{N}(y_i^* - \overline{y}^*)(y_i - \overline{y})}{\sqrt{\sum_{i=1}^{N}(y_i^* - \overline{y}^*)^2}\sqrt{\sum_{i=1}^{N}(y_i - \overline{y})^2}} \quad (1)$$

$$RMSE = \sqrt{\frac{1}{N}\sum_{i=1}^{N}(y_i - y_i^*)^2} \quad (2)$$

where:

y_i^* = predicted values.

y_i = actual values.

$\overline{y_i^*}$ and $\overline{y_i}$ = corresponding averages.

The models are well-trained and their performance increases with the data quality. Figure 6 shows the linear correlation between the predicted UCS using the ML models on the test set and the actual values. Comparing the performance of the models, it can be concluded that the SVR model obtained the worst performance (lowest correlation coefficient R = 0.95). However, the GBR and XGBR models exhibit a better fitting (and highest correlation coefficient R > 0.95) and can be generalised to be used on new data that they have never encountered before. This can be explained by the fact that algorithms based on DT and the boosting method are usually better performing in the prediction of tabular data. Moreover, the GBR model has the highest correlation coefficient (R = 0.99) due to its optimisation algorithm which is based on gradient descent where the errors of previous trees are corrected by the next ones (Mathivet 2021).

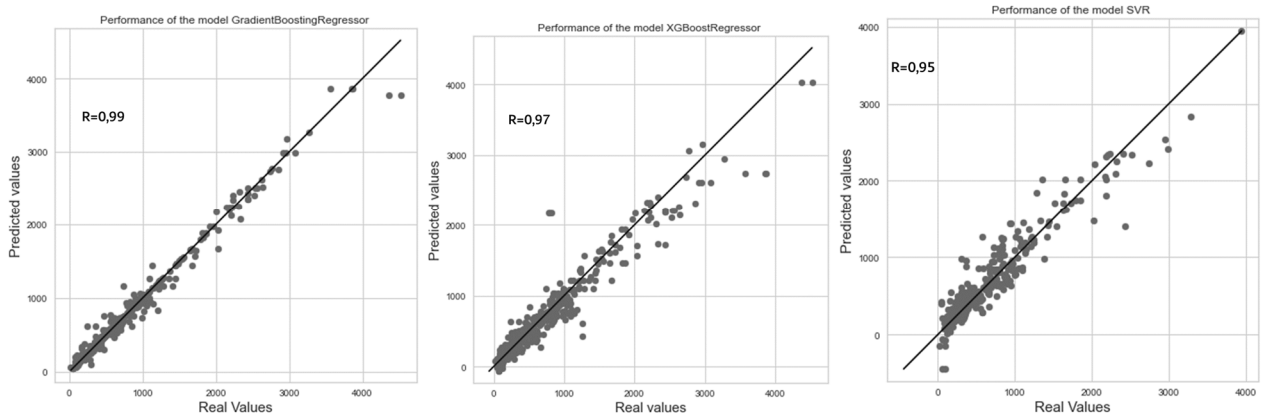

Figure 6 Comparison on the 1:1 line of the predictions obtained by the machine learning models and the actual values

The comparison between the predicted UCS by the models on the test data and the actual values is presented in Figures 7, 8 and 9. Low RMSE values of 0.16 and 0.17 were obtained with the GBR and XGBR models, respectively, while the SVR model is still the least efficient (Table 5).

To validate the evaluation of these models, three CPB mixtures were prepared in the laboratory that do not exist in the dataset with the aim of predicting their UCS values. The prediction results of these three mixtures using the three ML models are presented in Figure 10. As noted on the test dataset, the GBR and XGBR models are the best performers in prediction with a low RMSE error, while the SVR model has a large RMSE error.

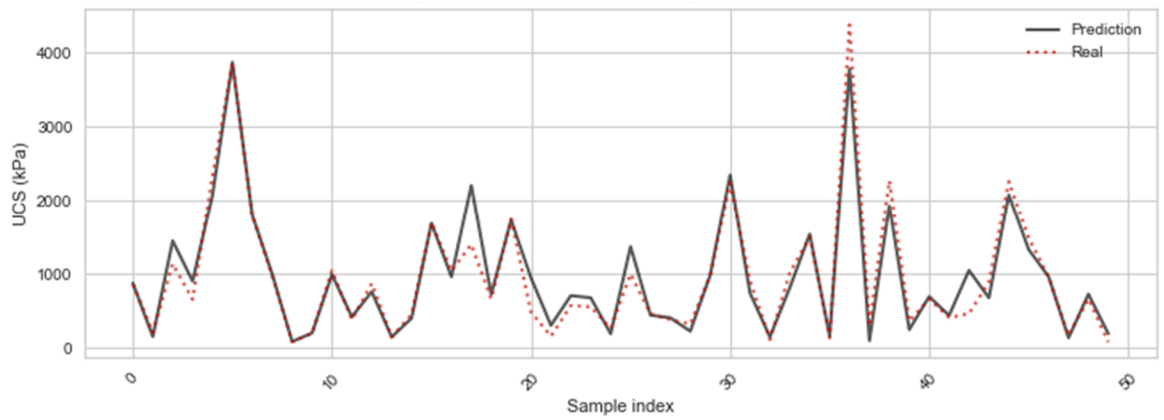

Figure 7 Comparison of actual UCS value and predicted UCS value using the GBR model

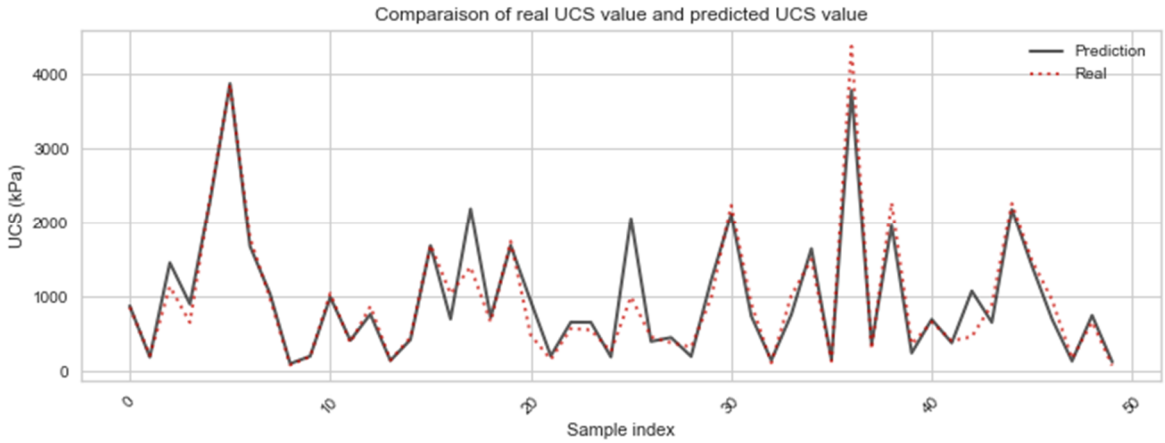

Figure 8 Comparison of actual UCS value and predicted UCS value using the XGBR model

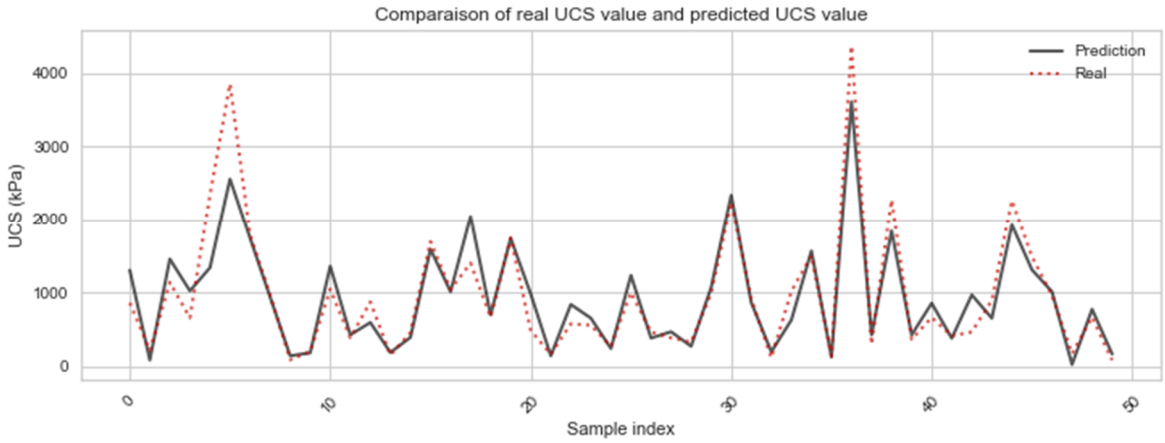

Figure 9 Comparison of real UCS value and predicted UCS value using the SVM model

Table 5 Performance of machine learning models

Parameter	Model (algorithm)		
	SVR	XGBR	GBR
R	0.95	0.97	0.99
RMSE	0.84	0.17	0.16

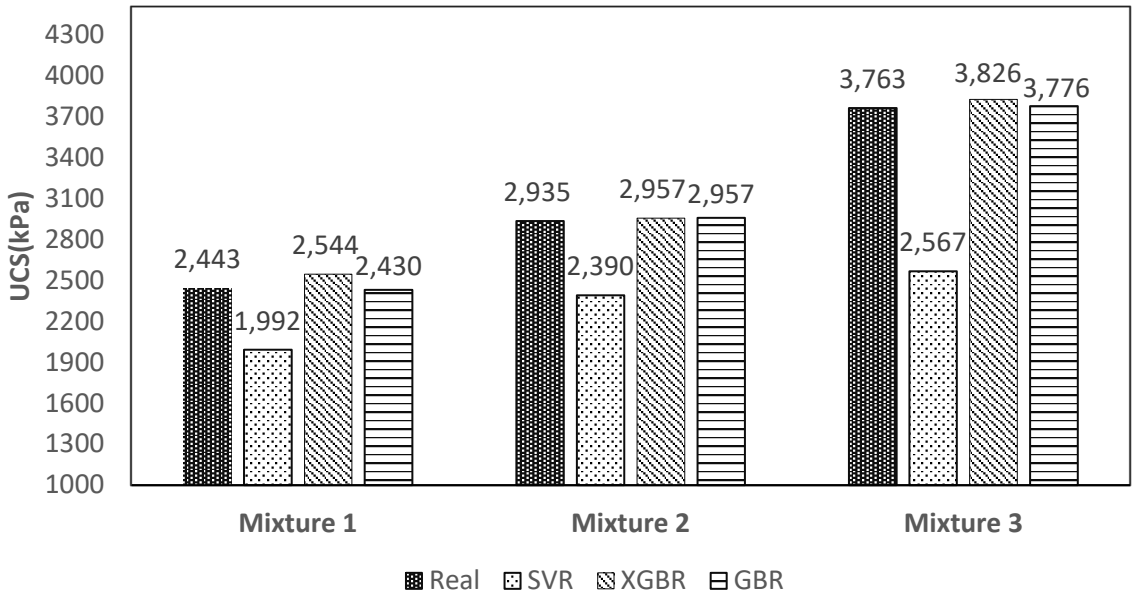

Figure 10 A comparison of the UCS prediction results using the three ML models

4 Conclusion

In this paper, three ML models were trained on a dataset including 1,587 uniaxial compression tests data taking into consideration the physicochemical properties of the tailings, the type and proportion of the binder, the solids mass concentration, the slump of the final paste, the mixing water quality, and the curing time. A pre-processing of data was done before training the models using the robust scaler method for data scaling. A cross-validation has been performed to determine the model hyperparameters and to avoid over-fitting and under-fitting.

Evaluation and validation of the model's performance were completed by preparing new CPB mix recipes in the laboratory to determine the corresponding UCS values and to compare them with those obtained using the ML models.

The results of this study show that:

- The interquartile range-based data normalisation method is effective in improving model learning and avoiding the effect of outliers.
- Optimisation of the model hyperparameters was done using the random search method with a number of iterations (*n_iter* = 10) followed by a 4-fold cross-validation.
- The best performance (described by the correlation coefficient R and RMSE error) was obtained by using the GBR model.
- Laboratory-scale prediction validation shows that the GBR model can accurately predict the UCS of CPB.

Acknowledgement

The authors would like to thank their university, UQAT and the Government of Canada for their financial support through the Research and Creation Grants – Support for the realisation of short projects (#FIRC/FUQAT 2021-2022), and the NSERC Discovery Grant (#RGPIN-2019-04946), respectively. The authors would also like to acknowledge the AEM Ltd for their partnership and financial support through the Research Institute of Mines and Environment.

References

Arioglu, E 1984, 'Design aspects of cemented aggregate fill mixes for tungsten stoping operations', *Mining Science and Technology*, vol. 1, no. 3, pp. 209–214.

ASTM International 2020, *Standard Test Method for Slump of Hydraulic-Cement Concrete (ASTM C143/C143M-20)*, ASTM International, West Conshohoken.

ASTM International 2021, *Standard Test Method for Compressive Strength of Cylindrical Concrete Specimens (ASTM C39/C39M-21)*, ASTM International, West Conshohoken.

Belem, T, Benzaazoua, M & Bussière, B 2003, 'Use of paste backfill as ground support. Part I: From its manufacture to its placement underground, *Proceedings International Symposium on Post-mining*, GISOS, Nancy, pp. 5-7.

Ercikdi, B, Yılmaz, T & Külekci, G 2014, 'Strength and ultrasonic properties of cemented paste backfill', *Ultrasonics*, vol. 54, no. 1, pp. 195-204.

Jakobowicz, E 2021, *Python for the Data Scientist: From Language Basics to Machine Learning*, 2nd edn, Dunod, Malakoff Cedex.

Lamos, A & Clark, I 1989, 'The influence of material composition and sample geometry on the strength of cemented backfill', in FP Hassani, MJ Scoble & TR Yu (eds), *Innovations in Mining Backfill Technology*, AA Balkema Publishers, Brookfield, pp. 89–94.

Landriault, DA, Verburg, R, Cincilla, W & Welch, D 1997, *Paste Technology for Underground Backfill and Surface Tailings Disposal Applications*, Canadian Institute of Mining and Metallurgy, technical workshop notes, vol. 27, 30 p.

Lu, X, Zhou, W, Ding, X, Shi, X, Luan, B & Li, M 2019, 'Ensemble learning regression for estimating unconfined compressive strength of cemented paste backfill', *IEEE Access*, vol. 99, pp. 7212572133.

Mathivet, V 2021, *Machine Learning: Implementation in Python using Scikit-Learn*, Editions ENI, Paris.

Mitchell, RJ & Wong, BC 1982, 'Behaviour of cemented tailings sands', *Canadian Geotechnical Journal*, vol. 19, no. 3, pp. 289–295.

Nelson, M & Illingworth, W 1991, *A Practical Guide to Neural Nets,* Addison-Wesley Publishing Co. Inc., Reading.

Nguyen, QH, Ly, HB, Ho, LS, Al-Ansari, N, Le, HV, Tran, VQ, Prakash, I, Pham, BT 2021, 'Influence of data splitting on performance of machine learning models in prediction of shear strength of soil', *Mathematical Problems in Engineering*, vol. 2021, article ID 4832864.

Ouattara, D 2017, *Experimental Study of the Rheological and Mechanical Properties of Cemented Paste Mining Backfills Incorporating Superplasticizers*, PhD thesis, Université du Québec en Abitibi-Témiscamingue, Rouyn Noranda.

Pham, BT, Hoang, TA, Nguyen, DM & Bui, DT 2018, 'Prediction of shear strength of soft soil using machine learning methods', *Catena*, vol. 166, pp. 181–191.

Qi, C, Fourie, A & Chen, Q 2018a, 'Neural network and particle swarm optimization for predicting the unconfined compressive strength of cemented paste backfill', *Construction and Building Materials*, vol. 159, pp. 473–478.

Qi, C, Chen, Q, Fourie, A & Zhang, Q 2018b, 'An intelligent modelling framework for mechanical properties of cemented paste backfill', *Minerals Engineering*, vol. 123, pp. 16–27.

Sahi, A 2016, *Experimental Validation of an Optimal Binder Selection Model in the Formulation of Cemented mine backfill mix designs*, master's thesis, Polytechnique Montreal.

Sun, Y, Li, G, Zhang, J, Sun, J & Xu, J 2020, 'Development of an ensemble intelligent model for assessing the strength of cemented paste backfill', *Advances in Civil Engineering*, article ID 1643529.

Swan, G 1985, 'A new approach to cemented backfill design', *CIM Bulletin*, vol. 78, no. 884, pp. 53–58.

Yaseen, ZM, Tran, MT, Kim, S, Bakhshpoori, T & Deo, RC 2018, 'Shear strength prediction of steel fiber reinforced concrete beam using hybrid intelligence models: a new approach', *Engineering Structures*, vol. 177, pp. 244–255.

Yılmaz, T, & Ercikdi, B 2016, 'Predicting the uniaxial compressive strength of cemented paste backfill from ultrasonic pulse velocity test', *Nondestructive Testing and Evaluation*, vol. 31, no. 3, pp. 247–266.

Yu, T 1989, 'Some factors relating to the stability of consolidated rockfill at Kidd Creek', *Innovations in Mining Backfill Technology*, pp. 279–286.

Yu Z, Shi X-Z, Chen X, Zhou J, Qi C-C, Chen Q-S & Rao D-J 2021, 'Artificial intelligence model for studying unconfined compressive performance of fiber-reinforced cemented paste backfill', *Transactions of Nonferrous Metals Society of China*, vol. 31, no. 4, pp. 1087–1102.